ELSEVIER

Catalysis Today 33 (1997) 215–225

CATALYSIS TODAY

Photoreactions of ethanol and MTBE on metal oxide particles in the troposphere

H. Idriss, A. Miller, E.G. Seebauer *

Department of Chemical Engineering, University of Illinois, Urbana, IL 61801, USA

Abstract

Ethanol (EtOH) and methyl tert-butyl ether (MTBE) are finding increasing use as fuel additives because of governmental mandates, and the relative merits of each have therefore become the focus of intense debate. The ultimate fate of fugitive emissions of these species forms one aspect of this controversy, because EtOH has been implicated in reductions in air quality, while MTBE has been linked to human illness. Both species have been shown to photoreact rapidly on fly ash particles in urban atmospheres. This work reports kinetic studies as well as detailed surface and bulk characterizations of fly ash by XRD, XPS, and SEM/EDA. The active phases in fly ash are probably Fe and Ti oxides. Addition of water to the reactant gas in some cases more than doubled the reaction rate of EtOH, but hardly affected that rate of MTBE. To gain insight into the respective roles of Fe, Ti, and alkali metals, kinetics were also measured over alkali-modified TiO_2 (anatase). Addition of Na or Ca oxides shifted the reaction product of EtOH from total oxidation (CO_2) to partial oxidation (acetaldehyde).

Keywords: Fly ash; MTBE; Tropospheric chemistry; Photochemistry

1. Introduction

In an effort to understand atmospheric chemical reactions, atmospheric chemists have traditionally examined homogeneous gas-phase radical (mainly OH) reactions of natural as well as anthropogenic pollutants. Although in general this approach has been successful, several observations suggest that other pathways exist that may contribute significantly to the overall network. These observations include the stoichiometric reactions of nitrogen oxides with NaCl from sea salt [1–3] and the catalytic oxidation of oxides of nitrogen and sulfur on soot and fly ash [4,5]. However, only the reactions on sea salt appear to be fast enough (at dawn) to contribute to tropospheric chemistry. On the other hand, several hypotheses have been advanced postulating important solid–gas photocatalytic reactions of organics on the Earth's surface as well as in the troposphere (the lower atmosphere). Several facts support these hypotheses. First, both the Earth's surface and the troposphere contain substantial quantities of particulates having large surface areas. In fact, the suspended particles alone may have available for reaction areas up to ten times that of the Earth's surface (modeled as a smooth sphere) [6]. Second, many particulates comprise semiconducting metal oxides. The most abundant of

* Corresponding author.

PII S0920-5861(96)00122-8

them are Fe and Ti oxides (although Zn and V oxides also exist) [7]. These oxides have band gaps of 2–3 eV, well within the range of the energy of the solar light [8]. Third, organics such as alcohols, acids, and ethers require up to 5 eV for direct photochemical reactions, i.e., higher than the majority of solar energy reaching the troposphere [9].

Oxygenated fuel additives are now increasingly used in order to enhance octane number and decrease pollution. These oxygenates comprise either alcohols such as methanol and ethanol (EtOH), or ethers such as methyl tert-butyl ether (MTBE), and ethyl tert-butyl ether. Their concentrations in the troposphere (currently about 10 mg/m^3 for each species [10]) are expected to rise with increasing use. The relative merits of each of these fuel additives (alcohols and ethers) have sparked intense debate [11]. Fugitive emissions form one facet of the controversy. Ethanol has been linked to overall reductions in air quality [12], and specifically connected to increased concentration of the irritant peroxyacetyl nitrate [13]. MTBE has been linked to human illness [14]. Since the reactions of these oxygenates are widely known to occur on metal oxide surfaces [15], and since the troposphere contain considerable concentrations of metal oxides, atmospheric photocatalytic reactions should proceed. The oxides act as semiconductors, and excitation by light having energy greater than the bandgap results in the creation of electron-hole pairs. In the presence of electron acceptors such as adsorbed molecular oxygen from the atmosphere, O^- and/or O_2^- are formed [16] that in turn may react with adsorbed organics. If the semiconductor remains intact and the charge transfer to the adsorbed species is continuous and exothermic, the process is properly classified as heterogeneous photocatalysis [17].

Recently, we have investigated [18,19] the reactions of EtOH and MTBE on the surfaces of combustion-generated fly ash, which is an anthropogenic metal oxide semiconductor. We found that photocatalytic reactions indeed occur with rates that can compete with the OH radical rates. MTBE photoreactions on fly ash were fast enough to yield considerable amounts of formaldehyde in a polluted environment, where the loading of particulates can be as high as 1 mg/m^3 [8]. A principal contributor to the large heterogeneous effect involved a follow up process to the reaction of MTBE with OH radicals to yield tert-butyl formate (TBF). This compound is relatively inactive toward OH radicals [20,21] but reacts with fly ash to yield tert-butyl alcohol (TBA), which further reacts homogeneously to acetone and formaldehyde.

In the present work, the surface and bulk compositions of fly ash are investigated by X-ray diffraction (XRD), X-ray photoelectron spectroscopy (XPS), scanning electron microscopy (SEM), energy dispersive analysis (EDA), BET, and atomic absorption analysis. Humidity effects on the reaction kinetics are examined for MTBE and EtOH on fly ash as well as on its photoactive components, TiO_2 and Fe oxides. The effects of the alkalis Ca and Na on the photoreaction of EtOH is also investigated because fly ash contains significant amounts of mono and divalent alkali.

2. Experimental

Kinetics were measured in a quartz flow reactor charged with 25 mg of solid, unless otherwise indicated in the text. Photoexcitation came from a defocused 75 W Xe arc lamp. The ultraviolet photon flux was calibrated by standard methods [22] involving NO_2 decomposition to NO + O, the rate constant for which is 0.3 min^{-1} at a flux of about 1×10^{16} photons/cm^2s. Our flux fell a factor of 23 below a typical noontime midlatitude solar flux [23], or about 0.4×10^{15} photons/cm^2s. The rate constants were rescaled by this factor to yield numbers characterizing the actual troposphere. Reactants and reaction products (MTBE, isobutene, methanol, ethanol, acetaldehyde, TBA, and TBF) were followed primarily with a

Perkin Elmer Sigma 2000 gas chromatograph using a 2 m Chromosorb 102 column and flame ionization detection (FID). Typical analyte concentrations, on the order of $1\text{-}5 \times 10^{-10}$ mol/ml (a few ppm at atmospheric pressure), did not permit reliable quantitative measurements using a differentially pumped mass spectrometer. Thus, all reactants and products were quantified using FID with external standards except for formaldehyde. Since this product is not detected by FID, its relative concentration with respect to an internal reference was followed by the mass spectrometer. Reactions proceeded at 35°C (forced air cooling) and a relative humidity of 50%, unless otherwise indicated in the text.

Fly ash was collected from the precipitator of the University of Illinois coal-fired power plant, and was sieved and/or ground to an average diameter of 5–10 μm. XRD was followed using a Rigaku Giegerflux with a fine focus Cu tube (45 kV, 20 mA). SEM was performed using a Hitachi S800 (20 kV). The same instrument together with its standard software provided bulk composition (ca. 1 μm depth) of individual particles by EDA. Surface composition and chemical state were probed by XPS using a Physical Electronics model 5400 instrument with a Mg-Kα anode at 400 W. Compositions were computed using manufacturer-supplied sensitivity factors based on photoionization cross sections of the individual elements. Spectral energies were calibrated using adventitious carbon at 284.7 eV.

Lewis base sites on the solid were titrated by CO_2 adsorption [18] as follows. The reactor was charged with 500 mg of solid and flushed with dry He for one hour at 100°C to remove reversibly adsorbed water. Pulses of CO_2 were subsequently injected (1 ml/pulse), and the emerging CO_2 peak was monitored by gas chromatography using a thermal conductivity detector. Complete restoration of the integrated peak areas for the pulses indicated saturation.

Na/TiO_2 and Ca/TiO_2 model surfaces were prepared by impregnation of NaOH or $Ca(OH)_2$ into 100% anatase TiO_2 (11 m^2/g, Fisher). The surface density of Ti cations was measured by XPS, and the corresponding amount of alkali was added to obtain alkali Ti ratios of between 1.0 and 5.0. The solids were calcined at 500°C for 5 h. No noticeable change in the surface area was observed after this procedure.

3. Results

3.1. Characterization

Fig. 1 presents SEM and EDA data for fly ash particles. Spherical particles having diameters between 1 and 15 μm were observed, with the majority of them between 3 and 10 μm. Spherical shapes often characterize fly ash particles, which are in fact often hollow [24]. Irregularly shaped particles have also been observed, however. Variations in chemical composition from particle to particle were also observed. In general, however, all were composed of Si and

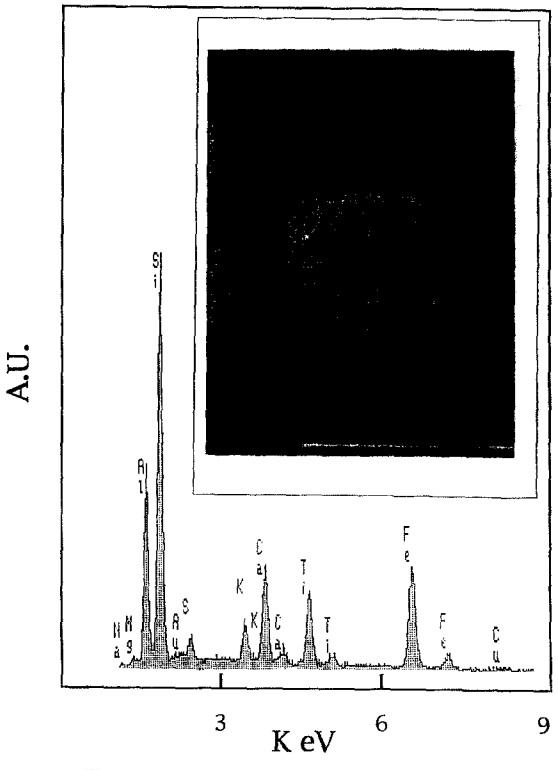

Fig. 1. SEM and EDA of one fly ash particle.

Al as major components, with non-negligible concentrations of transition metals (mainly Fe and Ti) together with alkali (Ca, K, and Na). The gold in Fig. 1 was added as an internal reference. XRD (not shown) indicated the presence of quartz, silica aluminates, magnetite, and hematite. Due to the interference of Ti (anatase) lines with silica aluminate and the low percentage of crystalline materials in fly ash (about 25 wt.% [25]), it was not possible to identify with good accuracy the Ti phases. (Ti anatase has its most intense line (101) at 3.5Å, and silica aluminate has its most intense line (110) at 3.4Å.) Quantitative analysis from EDA indicated that Ti and Fe represented about 4.4 and 13.5 atom%, respectively, of the overall surface concentration. Results were obtained by averaging over five typical particles. These concentrations contradicted those obtained by atomic absorption, particularly for Ti. Titanium had an overall concentration of about 0.5 atom%, indicating surface and near-surface enrichment of Ti with respect to the bulk. XPS was thus required in order to calculate overall surface and near-surface concentrations of transition metal oxides and to investigate their chemical states.

Fig. 2 presents an XPS survey scan of a broad surface of fly ash particles (about 10 mm diameter). Ti and Fe were present with concentrations of 3.4 and 25.7 atom%, respectively, confirming the EDA analysis. Non-negligible amounts of C, S, Ca, K, and Na were also present. Zn was not observed, eliminating ZnO and ZnS as potentially photoactive semiconductors. Sulphur is generally thought to exist in fly ash as gypsum ($CaSO_4$) [26]; SEM/EDA analysis showed some irregular crystals composed mainly of Ca and S, which might be those of $CaSO_4$. XPS of the Ti2p and Fe2p regions indicated that Ti and Fe existed in their highest oxidation state at the surface as evidenced by the $Ti2p_{3/2}$ line at 459.3 eV (Ti^{+4}) and $Fe2p_{3/2}$ at 712 eV (Fe^{+3}) [19]. Thus, from XRD, XPS, and SEM/EDA one may conclude that the fly ash surface consisted of Fe and Ti oxides coexisting with SiO_2, silica aluminate, and $CaSO_4$, liberally laced with alkali.

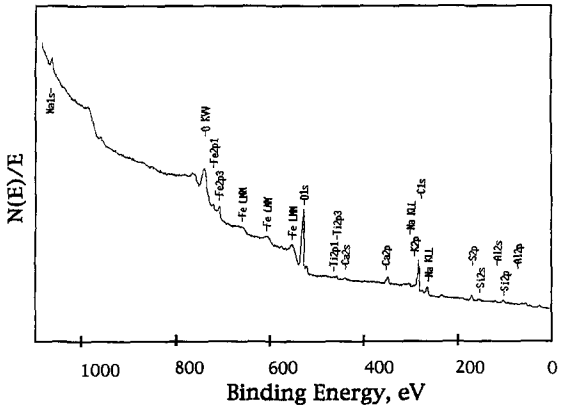

Fig. 2. XPS survey scan of a wide region of the fly ash surface.

Data concerning adsorption site characterization have been published previously for fly ash, Fe_2O_3, Fe_3O_4, and TiO_2 [19]. All surface areas fell in the range 7–11 m^2/g. Basic site densities for fly ash and the Fe oxides fell near 5×10^{18} sites/g, but were five-fold lower for TiO_2. EtOH adsorption was also conducted at room temperature to titrate overall adsorption capacity and yielded 20, 84, and 37×10^{18} molecules/g for fly ash, Fe_2O_3, and TiO_2, respectively.

3.2. Kinetics

Photoreaction kinetics of EtOH, MTBE, and TBF have been described previously [19]. TBF was examined because in the troposphere it results from the homogeneous reaction of MTBE with OH radicals [20]. The primary reaction products were as follows:

$$\underset{\text{EtOH}}{CH_3CH_2OH} \rightarrow \underset{\text{AcHO}}{CH_3CHO} + H_2, \quad (1)$$

$$\underset{\text{MTBE}}{(CH_3)_3COCH_3} \rightarrow \underset{\text{Isobutene(IB)}}{(CH_3)_2C=CH_2} + \underset{\text{Formaldehyde}}{HCHO} + H_2, \quad (2)$$

$$\underset{\text{TBF}}{(CH_3)_3COOCH} \rightarrow \underset{\text{TBA}}{(CH_2)_3COH} + CO/CO_2/H_2. \quad (3)$$

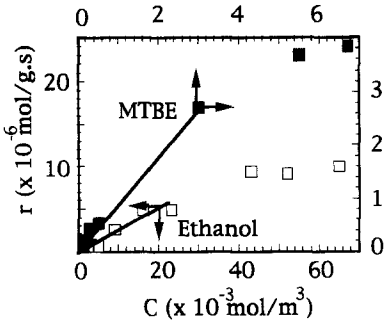

Fig. 3. Reaction rate as a function of reactant concentration for the photoreactions of MTBE and EtOH on fly ash.

In the reaction of MTBE, methanol also appeared as a minor product (< 5 mol%). Quantitative distinction between methanol and HCHO was made by comparing mass spectrometer peaks at m/e = 30 and 31 according to the method of Ko et al. [27].

Fig. 3 presents the rate of EtOH and MTBE photoreaction with fly ash as a function of reactant concentration, adapted from Ref. [19]. Two regimes are observed: a linear increase at low concentrations (first order) and saturation at high concentrations (zero order). This behavior is characteristic of Langmuir–Hinshelwood kinetics, which have been observed and studied in detail by several workers in connection with the photodecomposition of organics on TiO_2 in the gas and liquid phase [28,29]. This behavior permitted extrapolation of the rate from experimental conditions (ppm) down to the low concentrations (ppb) characterizing an actual urban troposphere. The rate expression obeys:

$$r = kKC/(1 + KC), \tag{4}$$

Table 1
Reaction rate constants

$kK\ 10^{-2}$ m^3/mg.day	EtOH	MTBE	TBF
Fly ash	1	8	20
Fe_2O_3	0.2	0.5	5
Fe_3O_4	0.1	0.7	2
TiO_2	11	12	7

(Adapted from Ref. [19]).

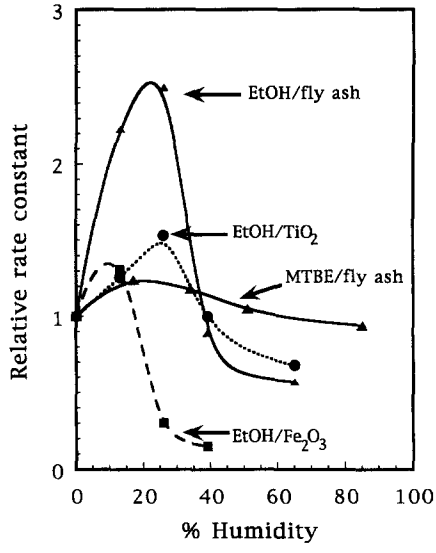

Fig. 4. Effect of humidity on the relative rate constant of EtOH and MTBE photoreactions on the surfaces of fly ash, Fe_2O_3, and TiO_2.

where r denotes the rate, K a binding constant, k a rate constant, and C the reactant concentration. Table 1 shows corresponding rate constants measured on fly ash and various pure oxides of Ti and Fe, adapted from Ref. [19]. SiO_2, Al_2O_3, and CaO were inactive.

3.3. Effects of humidity

Fig. 4 presents the effect of humidity on the relative reaction rate of EtOH and MTBE on fly ash, Fe_2O_3 and TiO_2. Three main points can be drawn from this figure. First, in all cases water enhanced to some extent the reaction rate up to humidities of 20–40%. This behavior is typical of a bimolecular surface reaction and can be expressed as follows:

$$r = k_o F_r F_w, \tag{5}$$

where

$$F_r = K_1 C_r/(1 + K_1 C_r + K_2 C_w), \tag{6}$$

$$F_w = K_4 C_w/(1 + K_3 C_r + K_4 C_w). \tag{7}$$

Here r denotes rate of reaction, k_o a rate constant, K_1 and K_4 binding constants, and C_r and

C_w the gas phase concentrations of the reactant and water, respectively [30]. The factors F_r and F_w represent competitive adsorption between the reactant and water for the same site. The increase of the reaction rate with water adsorption has been previously observed on TiO_2 [31] and was attributed to the creation of OH radicals formed upon H_2O dissociation followed by OH-recombination with a photogenerated hole. At high water concentrations, inhibition of the reaction rate resulted from surface site blocking. For both EtOH and MTBE, the effect of water on all three surfaces was totally reversible, in accord with reports of toluene oxidation on TiO_2 [30]. Second, the effects of humidity on fly ash and TiO_2 were similar, while on Fe_2O_3 the rate decreased more sharply and at lower humidity levels. Third, the effect of humidity on the reaction rate of MTBE with fly ash was the smallest, with almost no change in the reaction rate at humidity levels of 85% when compared to 0%. This result suggests that ethers do not compete extensively with water for the same sites. This conclusion may be tentatively rationalized by postulating that ethers initially adsorb nondissociatively through the oxygen lone-pair electrons, while water adsorbs by dissociation on a cation–anion pair site. Ethanol, which dissociates easily into a proton and alkoxide, should thereby compete fairly directly with water for sites, while MTBE should not.

Although the photoreaction of MTBE on fly ash is faster than that of EtOH [19], the following mechanistic study deals with EtOH photoreaction pathways mainly because its reaction products are simpler to follow. EtOH gives one product intermediate: AcHO, while MTBE gives three: isobutene, formaldehyde and methanol.

3.4. Reaction selectivity

Fig. 5 and Fig. 6 present the rate of EtOH photoreaction as a function of time (in batch) on TiO_2, Fe_2O_3, and fly ash. Two important points are indicated. First, the photoreaction of EtOH on TiO_2 is almost one order of magnitude faster

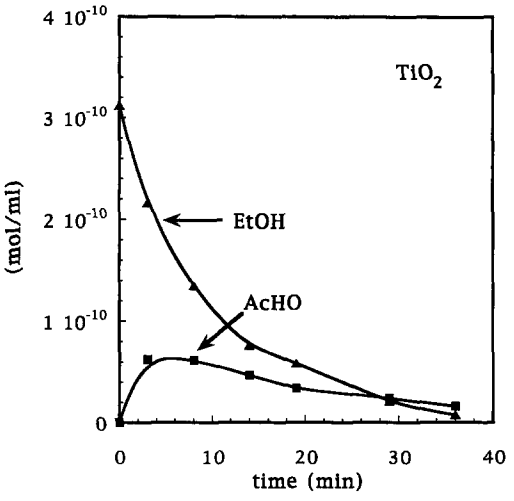

Fig. 5. Photoreaction of EtOH with TiO_2 (100% anatase, 11 m^2/g) as a function of time. Reactor volume: 250 ml, catalyst: 25 mg.

than that on Fe_2O_3, and about five times faster than that on fly ash. Second, while both fly ash and Fe_2O_3 yield acetaldehyde as a final product, TiO_2 further decomposes acetaldehyde into CO_2.

It is well accepted that the decomposition of oxygenates proceeds all the way to CO_2 on TiO_2 [28,29]. Clearly Fe_2O_3 does not oxidize acetaldehyde (with noticeable yield) further to CO_2. This considerable difference between the

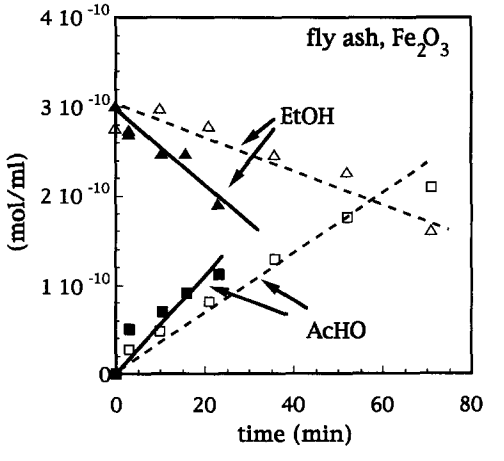

Fig. 6. Photoreaction of EtOH with fly ash (7 m^2/g, solid lines) and Fe_2O_3 (10 m^2/g, dashed lines) as a function of time. Reactor volume: 250 ml, catalyst: 25 mg.

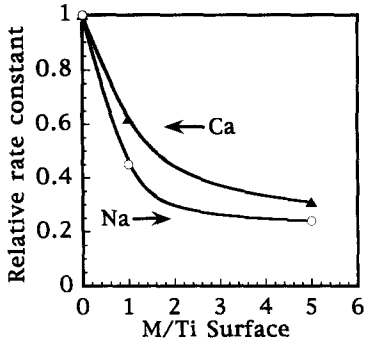

Fig. 7. Relative rate constant of the photoreaction of EtOH on M/TiO_2 (M = Na, Ca) as a function of M/Ti surface ratio.

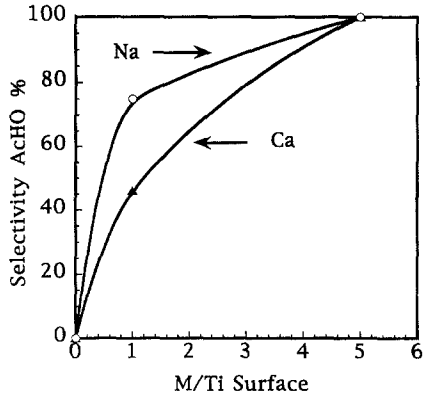

Fig. 8. Selectivity to AcHO of the photoreaction of EtOH on M/TiO_2 (M = Na, Ca) as a function of M/Ti surface ratio.

photoxidation on TiO_2 and on Fe_2O_3 might arise from the inability of Fe oxide to break C–C or C–O bonds (both Fe_2O_3 and Fe_3O_4 behaved similarly in our experimental conditions). Since, as shown in Fig. 6, both Fe oxides and fly ash partially oxidized EtOH to AcHO, one is tempted to conclude from this observation alone that the active phases on fly ash are those of Fe oxide. However two important other observations indicate otherwise. First, as seen from Table 1 and Fig. 6, the rate constant of EtOH on fly ash is faster than on pure Fe oxides (both surfaces have comparable surface areas). Second, as shown below, alkali-modified TiO_2 exhibits reactivity different from pure TiO_2.

3.5. Effects of alkali addition

Fig. 7 and Fig. 8 present the relative reaction rate and reaction selectivity, respectively, for EtOH photoreactions on TiO_2, Na/TiO_2, and Ca/TiO_2. Several observations can be drawn from these two figures. First, addition of Na or Ca decreased the reaction rate. It has also been observed recently that sodium oxide decreases the photoactivity of TiO_2 (anatase) towards the decomposition of stearic acid [32]. The most plausible explanation is site blocking on the surface of TiO_2 by sodium oxides. Second, addition of Na or Ca shifted the reaction selectivity completely from total oxidation to partial oxidation. This second observation reinforces the site-blocking explanation for the first. Since in order to achieve total oxidation multiple sites are required [33], blocking of some sites could result in partial reaction on the surface. The combination of these results with those from pure metal oxides and fly ash (Figs. 5–8) indicates that TiO_2 in fly ash might well provide the active sites along with Fe oxides. One cannot draw direct conclusions from comparison with individual pure components separately.

3.6. Effect of reaction temperature

Fig. 9 shows the effect of reaction temperature on the photoreaction (as well as the dark reaction) of EtOH with fly ash, Fe_2O_3, and TiO_2. The rate constant of the dark reaction (which yielded only acetaldehyde as final prod-

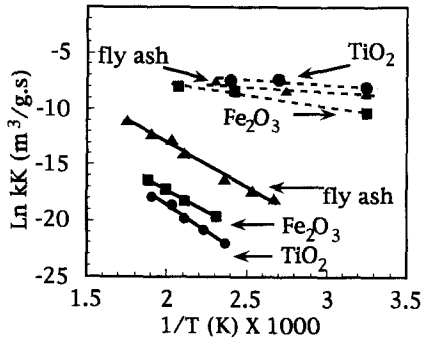

Fig. 9. Arrhenius plot (ln kK $m^3/g.s$ versus 1/T (K)) for the dark reaction (solid lines) and photoreaction (dashed lines) of EtOH on fly ash, TiO_2, and Fe_2O_3.

uct on all studied surfaces) on fly ash was higher by far than those of TiO_2 and Fe_2O_3, either per weight or per surface area. This enhancement on fly ash might be due to non-negligible amounts of CaO, which is also active for the oxydehydrogenation of EtOH to AcHO (E_a(CaO) = 11 kcal/mol) [34]. On the other hand, the Arrhenius plots of the photocatalytic reactions on all the surfaces were very close:

$$kK(\text{flyash}) = 6.5 \times 10^{-3}\exp[-2.3(\text{kcal/mol})/RT(K)], \quad (8)$$

$$kK(TiO_2) = 4.0 \times 10^{-3}\exp[-1.5(\text{kcal/mol})/RT(K)], \quad (9)$$

$$kK(Fe_2O_3) = 28 \times 10^{-3}\exp[-4.1(\text{kcal/mol})/RT(K)]. \quad (10)$$

The activation energies have standard error bars of roughly 0.5 kcal/mol. The pre-exponential factors and activation energies on fly ash and TiO_2 are very similar, while on Fe_2O_3 both quantities are noticeably higher. The low activation energies and pre-exponential factors seen in Eqs. (8)–(10) are typical of photoreactions [35].

4. Discussion

Several questions arise from this work. First, what are the implications of the photocatalytic reactions of oxygenates on their overall reactions in atmospheric environment? Second, what are the active phases on fly ash and related atmospheric solid particulates?

In order to answer the first question, one needs to compare the photocatalytic reaction of these two oxygenates to that of the radical reactions with OH in atmospheric conditions. This comparison appears for MTBE in Fig. 10, adapted from Ref. [19]. The numbers correspond to formation rates of products (in ppb/day) assuming an MTBE concentration of 10 ppb [10], an OH concentration of 2×10^6 molecules/ml [36], and a fly ash concentration of 0.5 mg/m^3 (50% of the total particulate loading in a polluted urban environment [8]). Published gas-phase rate constants [37] and branching ratios appear implicitly in the homogeneous calculations. The homogeneous reaction of MTBE proceeds through a sequence of steps to yield 2-methoxy, 2-methyl propanal (MMP) and TBF according to [20]:

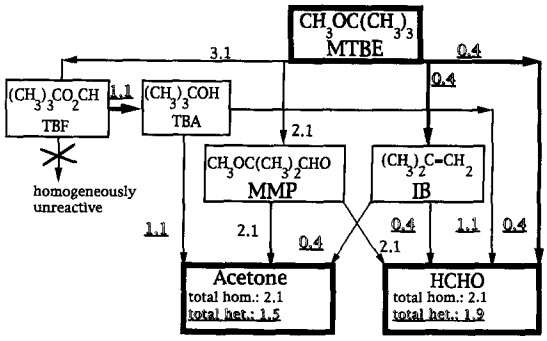

Fig. 10. Reaction scheme for MTBE by heterogeneous (dark lines) and homogeneous (light lines) pathways. Numbers correspond to formation rate of product (in ppb/day). The formation rates of both formaldehyde and acetone by pathways including at least one heterogeneous step roughly match those from purely homogeneous pathways. Adapted from Ref. [19].

$$\underset{\text{MTBE}}{(CH_3)_3COCH_3} + OH \rightarrow 0.4\underset{\text{MMP}}{CH_3OC(CH_3)_2CHO} + 0.6\underset{\text{TBF}}{HCOOC(CH_3)_3}. \quad (11)$$

The corresponding overall rate constant for MTBE disappearance is 0.6×10^{-6} s^{-1}. The initial heterogeneous conversion of MTBE runs about 15% as fast as the homogeneous one. However, TBF (considered relatively inert towards OH [20,21]) generated from the initial homogeneous step reacts rapidly on fly ash to yield TBA. All pathways ultimately end with formaldehyde and acetone, making for a convenient point to terminate the comparison. In the end, the contribution from pathways containing

a heterogeneous step roughly equal contributions from purely homogeneous pathways.

For EtOH, both homogeneous and heterogeneous reactions yield acetaldehyde directly. However, the computed homogeneous rate (6.8×10^{-6} s^{-1}) is about 80 times faster than the heterogeneous one (0.85×10^{-7} s^{-1}, from Table 1) at about 50% humidity although it decreases to about 30 times at 30% humidity (since the relative rate for EtOH at 30% humidity is about 2.5 times that at 0 or 50% humidity, Fig. 4).

To our knowledge the estimate for MTBE provides the first evidence yet for the importance of a catalytic reaction in the troposphere outside of a smoke plume. While the end product acetone is fairly benign, formaldehyde is toxic, corrosive, and carcinogenic [38]. At least with respect to aldehyde formation (formaldehyde in the case of MTBE and acetaldehyde in the case of EtOH) EtOH seems to carry some advantage over MTBE (since its heterogeneous photocatalytic reactions are less important than those of MTBE).

It is very difficult to address the second question and identify the active phases on a surface as complicated as fly ash. The following facts are worth collecting in one place in order to make progress.

(1) The fly ash surface contains substantial amounts of Fe and Ti oxides (Fig. 1 and Fig. 2), both of which are photoactive.

(2) The Fe oxides are present in both hematite (Fe_2O_3) and magnetite (Fe_3O_4) forms (XRD).

(3) Both the Ti and the Fe cations on the surface and in the near surface are in their highest oxidation state (Ti^{+4}, and Fe^{+3}) (XPS) [19].

(4) The fly ash surface contains a considerable number of Lewis basic sites (about 5×10^{18} sites/g) [19].

(5) While the photoreactions of MTBE (not shown) and EtOH (Fig. 5) on pure TiO_2 result in total oxidation to CO_2, those on Fe oxides and fly ash (Fig. 6) yield partial oxidation to acetaldehyde (for EtOH) and isobutene + formaldehyde (for MTBE).

(6) Doping the surface of TiO_2 with high amounts of Na or Ca results in shifting the reaction selectivity of EtOH from total oxidation (CO_2) to partial oxidation (acetaldehyde) (Fig. 7).

(7) The activation energies and pre-exponential factors for EtOH on both fly ash and TiO_2 are very similar while those on Fe_2O_3 are noticeably higher (Fig. 9).

The following comments may be made with respect to these facts. First, since Fe and Ti cations are in their highest oxidation state, it is possible to rule out oxidation state effects. That does not necessarily mean that lowering the oxidation state of some cations does not enhance the photoreaction, since it has been recently observed that the photoxidation of CH_3Cl on a partially reduced TiO_2 single crystal (which contains Ti^{+3}) proceeds more rapidly than on a fully oxidized one [39]. However, neglecting suboxide effects for fly ash does simplify the situation a bit. Second, both qualitatively and quantitatively one can also rule out any considerable difference between Fe_2O_3 and Fe_3O_4, since the two yield similar products with similar rates. Thus, at least with respect to Fe oxides it appears that photoxidation of EtOH and MTBE is structure-insensitive. This is not necessarily the case on TiO_2, where it is well accepted that the rutile phase is less active than the anatase phase for photoxidation reactions [28,29]. (However, the TiO_2 P25 Degussa catalyst which contains both phases (ca 70% anatase and 30% rutile) is a very active photocatalyst [40].) This being said, we prepared TiO_2 consisting of 40% rutile and 60% anatase (from $TiCl_4$ by precipitation with ammonia, BET = 49 m^2/g) and found no significant difference in either surface-area normalized rate or in constant product distribution when compared to the 100% anatase (11 m^2/g, Fisher). Third, doping TiO_2 with Ca and Na shifts the reaction products from total to partial oxidation. This is an important observation since fly ash photoreactions of EtOH, MTBE, and TBF also yield partial oxidation products.

Table 2
Reaction rate constant on fly ash

$kK\ 10^{-19}$ m^3/basic site.h			
	EtOH	MTBE	TBF
Observed	1.2	7.2	19.8
Calculated	4.0	4.4	6.1

(Adapted from Ref. [19]).

Taking these three points together suggests that both Fe and Ti cations together with alkali most likely contribute in the reaction. Dark dehydrogenation (or partial oxidation) of oxygenates usually requires Lewis basic sites [41]. Since the reaction products on fly ash signify dehydrogenation one may, by analogy, consider Lewis basic sites formed of Fe and Ti oxides to be the photoactive centers. The presence of alkali would enhance the basicity [42]. Fly ash, Fe and Ti oxides surfaces contain considerable amount of Lewis basic sites (sites titrated by CO_2) [19]. If one considers the surface atom density of Fe and Ti on fly ash together with their respective rate constants from pure-component oxide experiments, one can estimate the rate constant for fly ash. Such estimates appear in Table 2, which shows kK normalized by the basic site density in units m^3/site h. The calculated value reflects the rate constant obtained by dividing kK for each of the pure oxides TiO_2 and Fe_2O_3 by their respective basic site densities and summing the results according to the Fe and Ti densities on fly ash (obtained by XPS). The sum of these latter equals the experimental basic site density within 20%. This crude model reproduces the observed kK within a factor of three, and suggests that Ti accounts for up to 90% of the total reactivity even though Ti represents only 15% of the surface transition metal.

However, this approach does not give the right answer precisely. This most likely signifies a synergistic effect between Fe, Ti, and probably alkali. In fact, for the photoxidation of EtOH a synergistic effect between Fe_2O_3 and TiO_2 has been observed [34]; a 30% Fe–70% Ti mixture (at the surface) was 1.5 and 4 times more active than the pure TiO_2 and Fe_2O_3, respectively.

5. Conclusion

Important implications follow from this work. Since oxides catalyze reactions of volatile organic compounds, the effects of these solids on the overall tropospheric reaction network merit further investigation. The active phases in fly ash appear to be Fe and Ti oxides together with alkali (such as Ca and Na). The results presented here suggest that particulate composition, particularly with respect to Fe and Ti, may be considered in pollution control strategies to enhance CO_2 at the expense of noxious aldehydes.

Acknowledgements

EGS gratefully acknowledges a Sloan Foundation Fellowship. This work was partially supported by the National Science Foundation under a Presidential Young Investigator Award.

References

[1] B.J. Finlayson-Pitts, M.J. Ezell and J.N. Pitts, Jr., Nature, 337 (1989) 241.
[2] J.M. Laux, J.C. Hemminger and B.J. Finlayson-Pitts, Geophys. Res. Lett., 21 (1994) 1623.
[3] F.E. Livingston and B.J. Finlayson-Pitts, Geophys. Res. Lett., 18 (1991) 17.
[4] T. Novakov, S.G. Chang and A.B. Harker, Science, 186 (1974) 259.
[5] R. Dluji and H. Gusten, Atm. Environ., 17 (1983) 1765.
[6] W. Jaeschke, Nato ASI Series. Series G: Ecological Sciences, 6 (1986) 567.
[7] S. Sharma, M.H. Fulekar and C.P. Jayalakshmi, Crit. Rev. Environ. Contr., 19 (1989) 251.
[8] J.H. Seinfeld, Atmospheric Chemistry and Physics of Air Air Pollution, Wiley, New York, 1986, p. 445.
[9] K.I. Zamaraev, M.I. Khamov and V.N. Parmon, Catal. Rev.-Sci. Eng., 36 (1994) 617.
[10] T.J. Kelly, R. McRund, C.W. Spicer and A.J. Pollack, Environ. Sci. Technol., 28 (1994) 378A.
[11] Chem. and Eng. News (1994) 8.

[12] L.M. Thomas, Cong. Digest, February 1989, p. 43.
[13] R.L. Tanner, A.H. Miguel, J.B. de Andrade, J.S. Gaffney and G.E. Streit, Environ. Sci. Technol., 22 (1988) 1026.
[14] J.P. Middaugh, Science, 263 (1994) 1545.
[15] H. Idriss, M. Libby and M.A. Barteau, Catal. Lett., 15 (1992) 13.
[16] M. Anpo and Y. Kubokawa, J. Phys. Chem., 88 (1988) 5556.
[17] A.L. Linsbigler, G. Lu and J.T. Yates, Jr., Chem. Rev., 95 (1995) 735.
[18] H. Idriss and E.G. Seebauer, submitted to Environ. Sci. Technol.
[19] H. Idriss and E.G. Seebauer, J. Vac. Sci. Technol. A., in press.
[20] S.M. Japar, T.J. Wallington, J.F.O. Richert and J.C. Ball, Int. J. Chem. Eng., 22 (1990) 1257.
[21] R.A. Harley, G.R. Armistead, G.J. McRace, G.L. Cass and J.H. Seinfeld, Environ. Sci. Technol., 27 (1993) 278.
[22] S. Kutsuma, Y. Ebihara, K. Nakamura and T. Ibuzuki, Atm. Environ., 27A (1993) 559.
[23] J.H. Seinfeld, Atmospheric Chemistry and Physics of Air Air Pollution, Wiley, New York, 1986, p. 113.
[24] N. Shigemoto, H. Hayashi and K. Miyaura, J. Mat. Sci., 28 (1993) 4781.
[25] S.C. White and E.D. Case, J. Mat. Sci., 25 (1990) 5215.
[26] Y. Xie, P.K. Hopke and D. Wienke, Environ. Sci. Technol., 28 (1994) 1921.
[27] E.I. Ko, J.B. Benziger and R.J. Madix, J. Catal., 62 (1980) 264.
[28] M.A. Fox and M.T. Dulay, Chem. Rev., 93 (1993) 341.
[29] M.R. Hoffmann, S.T. Martin, W. Choi and D.W. Bahnemann, Chem. Rev., 95 (1995) 69.
[30] N.T. Obee and R.T. Brown, Environ. Sci. Technol., 29 (1995) 1223.
[31] J. Peral and D.F. Ollis, J. Catal., 136 (1992) 554.
[32] Y. Paz, Z. Luo and A. Heller, 42nd National Symposium of American Vacuum Society, October 16–20, 1995, Paper no: TF-FrM9.
[33] M.L. Sauer, M.A. Hale and D.F. Ollis, J. Photochem. Photobio. A: Chemistry, 88 (1995) 169.
[34] H. Idriss, A. Miller and E.G. Seebauer, to be published.
[35] A. Mills, R.H. Davies and D. Worsley, Chem. Soc. Rev. (1993) 417.
[36] A.T. Thompson, Israel J. Chem., 34 (1994) 277.
[37] R. Atkinson, D.L. Bauch, R.A. Cox, R.F. Hampson, Jr., J.A. Ken and J. Troy, Int. J. Chem. Kinet., 21 (1989) 115.
[38] A.P. Altshuller, Atm. Environ., 27A (1993) 21.
[39] G. Lu, A. Linsbebigler and J.T. Yates, Jr., J. Phys. Chem., 99 (1995) 7626.
[40] R.W. Mattheus, J. Catal., 111 (1988) 264.
[41] A.L. McKenzie, C.T. Fishel and R.J. Davis, J. Catal., 138 (1994) 1921.
[42] H. Hattori, Chem. Rev., 95 (1995) 537.